

TITLE: SIMPLE DFT-LSDA MODELLING OF THE MOLECULAR-LIKE ASPECTS OF ULTRA-THIN FILM PROPERTIES

AUTHOR(S): Samuel B. Trickey, U. of Florida, Gainesville, FL.
Richard J. Matthar, U. of Florida, Gainesville, FL.
Jonathan Carl Boettger, Theoretical Division, T-1, LANL

SUBMITTED TO: Proceedings of the Third-UNAM-CRAY Supercomputing Conference on Computational Chemistry (Mexico City, Mexico)

MASTER

By acceptance of this article, the publisher recognizes that the U.S. Government retains a nonexclusive, royalty-free license to publish or reproduce the published form of this contribution, or to allow others to do so, for U.S. Government purposes.

The Los Alamos National Laboratory requests that the publisher identify this article as work performed under the auspices of the U.S. Department of Energy.

Los Alamos Los Alamos National Laboratory
Los Alamos, New Mexico 87545

DISCLAIMER

**Portions of this document may be illegible
in electronic image products. Images are
produced from the best available original
document.**

DISCLAIMER

This report was prepared as an account of work sponsored by an agency of the United States Government. Neither the United States Government nor any agency thereof, nor any of their employees, makes any warranty, express or implied, or assumes any legal liability or responsibility for the accuracy, completeness, or usefulness of any information, apparatus, product, or process disclosed, or represents that its use would not infringe privately owned rights. Reference herein to any specific commercial product, process, or service by trade name, trademark, manufacturer, or otherwise does not necessarily constitute or imply its endorsement, recommendation, or favoring by the United States Government or any agency thereof. The views and opinions of authors expressed herein do not necessarily state or reflect those of the United States Government or any agency thereof.

Simple DFT-LSDA Modelling of the Molecular-like Aspects of Ultra-thin Film Properties

By S.B. TRICKEY¹,
R.J. MATHAR¹, AND J.C. BOETTGER²

¹Quantum Theory Project, Univ. of Florida, Gainesville, FL 32611-8435, USA

²Theoretical Division, Los Alamos National Laboratory, Los Alamos, NM 87545, USA

Ordered ultra-thin Films (UTF's) are atomic n -layers ($n = 1, 2, 3, \dots$) with translational symmetry in-plane and molecular-like inter-planar spacings. Though commonly used (especially at relatively large n -values) as models of crystalline surfaces, they are intrinsically interesting and of growing technological significance as the basic building blocks of multi-layer electronic devices. Predicting the structure and properties of even a simple diatomic 1-layer means addressing aspects of molecular binding (and boundary conditions) in the context of an extended, periodically bounded system. At the level of refinement provided by the local spin density approximation to Density Functional Theory, the baseline standard of today's predictive, chemically specific solid-state calculations, a number of technical and fundamental issues arise. We focus on treatment of the isolated atoms, on basis sets, and on numerical precision, as illustrated by the Fe atom and BN 1- and 2-layer calculations. Computational requirements are illustrated by a brief summary of recently completed calculations on crystalline sapphire, α -Al₂O₃, which used the same code.

1. Introduction

An ordered ultra-thin film (UTF) is a construct abstracted from real multi-layer systems in, for example, microelectronics. The abstraction is to assume a self-supporting system consisting of n ($n = 1, 2, 3, \dots$) planes of atomic nuclei, all with a common translational symmetry in-plane (x - y). The electronic structure problem, in the static lattice approximation, then has periodic boundary conditions with two-dimensional space groups in-plane and vacuum boundary conditions along both positive and negative z -axes. Even in-plane such a system may be rather molecular locally. For $n \geq 2$ but modest (say ≤ 20), the transverse electron distribution may be quite molecular in character or, as in BN, somewhat peculiar whether viewed from the molecular or crystalline perspective.

The tasks are to find the minimum energy static structure, predict the properties at that minimum, characterize the behavior of the sequence with growing n , and compare with the associated crystal. The state of the art for such predictive, chemically specific studies is to use Density Functional Theory (DFT). As is well known, to use DFT requires selection of an approximation to the exchange-correlation kernel. Elsewhere one of us [Trickey (1996)] has given evidence that gradient dependent approximations (GDA) are not yet well-enough understood to be used for predictive calculations if the intended audience includes a significant weighting of experimenters. Thus we use the local spin density approximation (LSDA) here. Although details would of course change, none of the main themes of the paper would be altered in any dramatic way were a GDA to have been used.

2. Problems with atoms

The first task in the list, determination of the cohesive energy E_{coh} , leads directly to a problem stated most succinctly, to our knowledge, by Dennis Salahub at the Aug. 1995 Paris DFT meeting: "in practical applications of DFT, atoms are hardest." That plain remark embodies several intertwined issues.

At the fundamental level, the essential localization of an atom means that self-interaction-error (SIC) [Perdew & Zunger (1981)] in LSDA, which is positive, cannot be reduced via delocalized Kohn-Sham (KS) states such as occur in aggregates. Technically, there is impact on computational schemes which use localized basis functions. To control systematic error, one needs to calculate the atomic total energies which enter E_{coh} with the same basis and associated algorithms. Use of an excessively compact basis set for the atom, however, will worsen the SIC error, hence artificially enhance the calculated binding of the extended system by making the atomic total energy too high. Since small basis sets are a common choice for extended systems, the risk is clear. (An excessively rich atomic basis will unbalance the calculation, admittedly, but it is rare to encounter that problem.)

Another fundamental point is that a key feature of the KS solution to the DFT variational problem is separation of the system kinetic energy into a large part (T_s , the contribution from the KS reference system) and a small part (in the exchange correlation term). Avoiding making T_s too high via too compact a basis set is a challenge that seems to be underappreciated, especially for the isolated atom. Third, inadequate basis set flexibility can lead to erroneous occupancies for the KS orbitals, with potentially serious consequences for both the energetics and the KS orbital eigenvalues. Fourth, cancellation of core contributions in the calculation of E_{coh} is a slippery business; a small imbalance between the cores of the aggregate and the separated constituents can result in a relatively large error in E_{coh} .

The Fe atom provides an apt illustration. From all-numerical calculations, it has long been known that, in LSDA (results here are for the Hedin-Lundqvist model, but the points are general), the Fe atom ground state in the central field approximation has fractional occupancy of the KS orbitals: $[\text{Ar}]3d_{\uparrow}^{5.0}3d_{\downarrow}^{1.4}4s_{\uparrow}^{1.0}4s_{\downarrow}^{0.6}$ [Moruzzi *et al.* (1978)]. Some time ago we heard of a gaussian basis calculation which found the lowest LSDA energy for the Fe atom to have *integer* occupation numbers. E_{tot} for the calculation appeared higher than plausible, however.

Beginning with a published $14s9p5d$ basis [Wachters (1970)], we used our gaussian orbitals atoms code GATOMS (which does coulomb integrals analytically and the LSDA XC integrals numerically) to study basis set enrichment effects upon the KS occupancy and total LSDA energy of the Fe atom. Indeed, the $14s9p5d$ basis gave $3d^64s^2$ KS occupation as lowest in energy. Systematic enlargement of the basis through $20s14p10d$ gave unequivocal KS fractional occupancies identical with the all-numerical results. Even at that very large basis, however, E_{tot} was more than 10 mRy above the all-numerical result. Finally, with a rationally tempered $20s16p12d$ (all un-contracted) basis of our own construction, the fractional occupancy total energies were

$$\text{Numerical ("exact")}: E_{\text{tot}} = -2522.369 \text{ Rydbergs}$$

$$\text{Gaussian basis}: E_{\text{tot}} = -2522.3593 \text{ Rydbergs}$$

Integer occupancies raised E_{tot} in the gaussian basis by 0.011 Rydberg.

We were unwilling to deploy an even larger basis in pursuit of the remaining 9.7 mRy in total energy, since that residue is an error more than an order of magnitude smaller than the shift in E_{tot} , about 0.11 Ry = 1.5 eV, from $14s9p5d$ to $20s14p10d$. Put this in context: a study [Boettger (1993)] of spin-dependent energetics of the Fe 1L used a

s-exponents	p-exponents	d-exponents
4445500.000000000	15102.000000000	1620.000000000
889100.000000000	5034.000000000	405.000000000
177820.000000000	1678.000000000	135.000000000
35564.000000000	745.777777000	45.000000000
8891.000000000	331.456780000	19.148936000
3783.404260000	147.314120000	8.148483400
1609.959260000	65.472942000	3.467439700
685.089046000	29.099085000	1.475506200
291.527254000	12.932926000	0.627874970
124.054150000	5.747967100	0.267180830
52.789002000	2.554652000	0.113693970
22.463404300	1.135400800	0.040000000
9.558895460	0.504622570	
4.067615090	0.224275669	
2.033807550	0.100000000	
1.016903770	0.040000000	
0.508451890		
0.133373150		
0.056754530		
0.024150860		

TABLE 1. 20s16p12d Gaussian basis for Fe atom

10s7p + 1p_z3d contracted basis built from a Huzinaga & Sakai (1969) 14s9p5d set with augmentations. Even that 1L basis set is rather larger than those commonly used in molecular and extended system DFT (or for that matter, Hartree-Fock) calculations.

As inspection of Table 1 will show, most of the investment in augmenting from 14s9p5d to 20s16p12d is to improve the representation of the cusp at the nucleus. Usually it is argued that such refinements in core electron orbitals are not significant for calculations of E_{coh} because of cancellation but it only takes a small failure of cancellation to yield potentially substantial errors in E_{coh} .

To summarize: in respect to basis sets, the thrust of Salahub's point is that every truncation error one makes easily can be in the wrong direction, with the resulting atomic energy driven upward and E_{coh} made artificially large in magnitude.

3. Ultra-thin films of hexagonal boron nitride

3.1. Background

Hexagonal boron nitride (*h*-BN) [Pease (1952)] is the natural crystalline state of a layered material isoelectronic with graphite. However, instead of being semi-metallic, *h*-BN is an insulator. The experimental and computational literature on *h*-BN is too extensive to review here. References beyond those found here are in, for example, Jia *et al.* (1996), Furthmüller, Hafner and Kresse [Furthmüller *et al.* (1995)], Wentzcovitch *et al.* (1988), and Causá *et al.* (1988). We focus particular attention on Nagashima *et al.* (1995) on the experimental side and upon Blase *et al.* (1995) and Catellani *et al.* (1986) on the computational side.

Nagashima *et al.* (1995) studied the *h*-BN monolayer deposited epitaxially (by thermal decomposition of borazine B₃N₃H₆) on Ni, Pd, and Pt(111) via angle-resolved electron spectroscopies and concluded that the electronic structure of the *h*-BN 1L "... is almost independent of the substrate" and hence that the system is a potentially important

example of a stable, weakly physisorbed overlayer. They also noted that “because of the strong reduction of the surface reactivity for borazine decomposition due to the monolayer BN coating, the growth rate of the following BN layers became extremely small ...”

Here we present results of all-electron, full-potential, non-relativistic LSDA calculations for the mono- and bilayers of *h*-BN to explore and illuminate those findings. The calculations are an application of the LCGTO-FF electronic structure techniques for solution of the KS problem as embodied in the program package GTOFF. For brevity the reader is referred to prior descriptions [Boettger (1995)]. This work differs from and is complementary to that of Blase *et al.* (1995) in several respects. Their monolayer was in fact a supercell calculation and they used pseudopotentials, whereas we treat true UTF's, include all electrons, and study both the 1L and 2L.

3.2. Basic experimental data

The experimental lattice parameters for *h*-BN at room temperature are $a = 4.732a_0$ and $c = 12.587a_0$ [Lynch & Drickamer (1966), Landolt & Börnstein (1982)], where a_0 is the Bohr radius. The B-N distance in the basal planes is a factor of $1/\sqrt{3}$ shorter than a , *i.e.* $2.732a_0$. The distance between layers is a factor of 2 shorter than c , whence the interplanar B-N distance is $6.294a_0$, a clear indicator of the weak interplanar binding. For comparison, molecular BN has a bond length of $r_e = 2.421a_0$ [Herzberg (1950)].

When traced to their origins, all known experimental results for E_{coh} of BN apparently refer to the hexagonal modification. Direct calculation from the CODATA [Cox *et al.* (1989)] tabulations yields an experimental, $T = 0$ K, $E_{\text{coh}} = -13.43$ eV/f.u. = -6.71 eV/atom. To correct for the zero-point vibrational energy, it is typical to use the Debye model [Lam *et al.* (1990)]. The relatively weak interplanar binding suggests exploitation of a planar Brillouin zone (BZ) and a two-dimensional Debye temperature [Dworkin *et al.* (1954), Landolt & Börnstein (1982)], which turns out to be 598 K. In contrast the three-dimensional Debye temperature was measured to be 323 K [Sichel *et al.* (1976)]. To circumvent the limitations of this model, we approximated a newer theoretical result of Nozaki & Itoh (1996) by easily integrable pieces, normalized the phonon density of states — the area under the curve — to be six, and obtained a zero point energy of 0.34 eV/f.u., which is half of the first moment of the function. The net result is a static lattice cohesive energy of -6.88 eV/atom.

3.3. Monolayer and bilayer results

The hexagonal UTF's have point group symmetry $D_{3h}(\bar{6}m2)$, as discussed, for example, by Doni & Parravicini (1969). The monolayer (bilayer) total energy calculations used a 30×30 (18×18) point mesh in the full hexagonal Brillouin zone. Once the equilibrium lattice parameters for the two systems were determined, comparison calculations were done to insure that the difference in the two BZ meshes do not introduce artificial energy differences between the two systems. Basis sets are tabulated in the Appendix.

Monolayer total energies were calculated at twelve values of the lattice parameter in the range $4.6019a_0 \leq a \leq 4.9319a_0$. All the resulting energies (in Hartree per formula unit) are fit almost exactly (indistinguishably on a page-sized plot) by the cubic expression $E_{\text{tot}} = -79.075872 + 0.204(a - 4.7197)^2 - 0.107(a - 4.7197)^3$. The location of the minimum agrees with the experimental bulk lattice constant to better than 0.3%. The calculated E_{coh} is -7.66 eV/atom (relative to spin-polarized, large basis LSDA values for B and N of -24.36296 and -54.14929 Hartrees respectively). The overbinding relative to experiment, by 0.78 eV/atom, is typical of published calculations for the bulk crystal, indeed not as severe as some. See Table VII of Furthmüller *et al.* (1995) for further comparison.

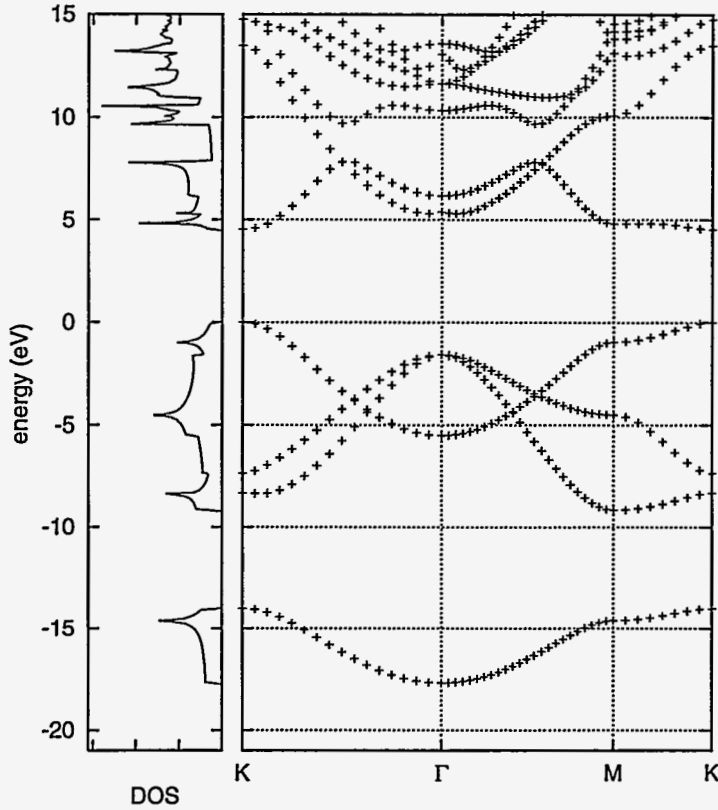


FIGURE 1. Energy bands (bare KS eigenvalues) and density of states for the BN monolayer at the theoretical equilibrium lattice constant $a = 4.7197a_0$.

The energy surface for the hexagonal bilayer was computed on a 7×7 grid with the lattice parameter a between $4.6319a_0$ and $4.8319a_0$ and lattice parameter c between $11.5374a_0$ and $13.0874a_0$. A 6-parameter least-squares fit of a second-order polynomial to the calculated energies yields (in Hartree per formula unit) $E_{\text{tot}} = -79.07785 + 0.198(a - 4.7220)^2 + 0.0000926(c - 11.908)^2 + 0.000330(a - 4.7220)(c - 11.908)$. The bilayer in-plane lattice parameter hence deviates from the experimental bulk lattice parameter by only 0.2%, but the bilayer interplanar equilibrium spacing is decreased by slightly more than 5%. If there is any LSDA lattice contraction in the bulk crystal (our calculations were incomplete at the time of writing), then the predicted decrease would, of course, be smaller.

E_{coh} for the bilayer is 0.027 eV/atom lower than for the monolayer, $E_{\text{coh}} = -7.69$ eV/atom, very close to the interplanar binding energy in graphite [Trickey *et al.* (1992)]. (By direct testing, the shift which results from use of different BZ scan densities in the mono- and bilayers was found to be two orders of magnitude smaller than the energy difference between the systems.) Note that this calculated energy difference is consistent with the relative difficulty of forming an epitaxial bilayer experimentally (recall the introductory summary to this section). In addition to the inhibited thermal decomposition of borazine discussed by the experimenters, there is very little energetic advantage to forming the bilayer since the deposition is done at 800 °C. For comparison, the calculated energy advantage of the bilayer over the monolayer is about 625 K per atom pair.

The intraplanar stiffness of the bilayer, as measured by the coefficient of the quadratic

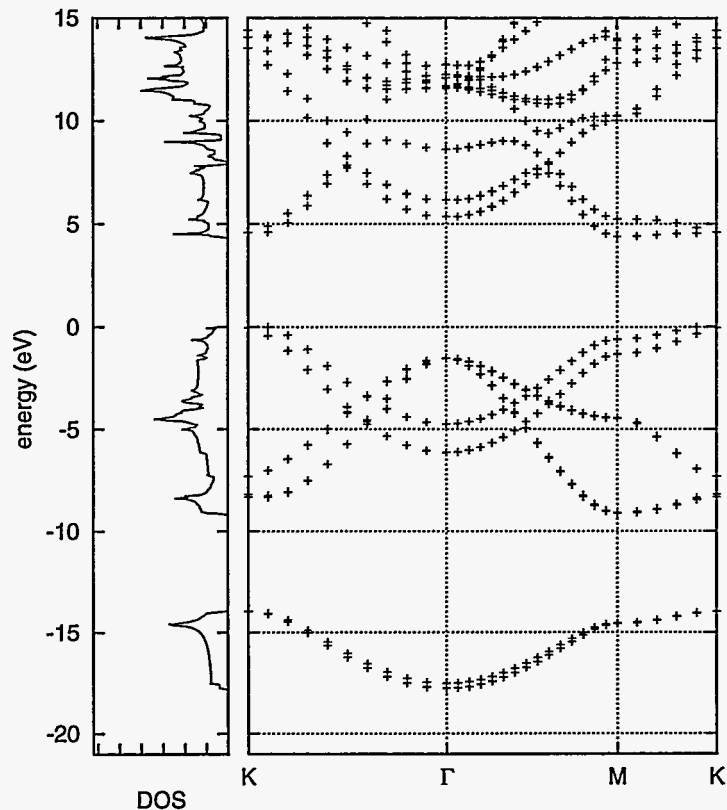


FIGURE 2. As in Fig. 1 for the BN bilayer. See Table 2 for bandwidth comparisons.

term in a , is about 5% larger than for the monolayer, if the energy of the monolayer is also fitted only up to $O(a^2)$. If the fitted quadratic form of the energy as a function of a and c is diagonalized, the eigenvector corresponding to the smaller eigenvalue has one positive and one negative component in the space spanned by the variables a and c . The corresponding physical meaning is that a path on the energy surface which starts from the theoretical equilibrium position and follows the direction of the smallest gradient lets a grow and c shrink or vice versa. This property leads to the correct behavior under uniaxial stress and places the energy minimum at larger a for smaller c .

The monolayer band structure (bare KS eigenvalues) at the calculated equilibrium lattice parameter but with 48×48 points in the full Brillouin zone is shown in Fig. 1. Band gaps and bandwidths are collected in Table 2. The monolayer is a direct gap semiconductor, with an LSDA gap of 4.51 eV at the K point. Allowing for the difference in LSDA models, the tables and figures in Blase *et al.* (1995) agree with this result (the text of that paper is not consistent with its tables and figures on this matter). There is a slight upward dispersion in the lower σ valence band beginning about 90% of the way out from Γ toward K, behavior which at least qualitatively is consistent with the experimental data of Nagashima *et al.* (1995), the calculations of Catellani *et al.* (1986) (crystal) and of Blase *et al.* (1995) (crystal and supercell monolayer).

The GW calculation of Blase *et al.* (1995) yields an estimate of the typical LSDA band-gap underestimation of 1.7 eV (we put aside the subtle question of whether the gap is shifted from direct to indirect in going from LSDA to GW). Allowing for that underestimate, the close resemblance between the LSDA energy bands for the free monolayer and

Authors	E_{gap}	W_{π}	W_{σ_1}	W_{σ_2}
Expt.	5.2	5.8	6.5	8.2
Present 1L	4.51	5.49	5.76	7.55
Present 2L	4.38	4.75, 6.13	5.78	7.60
Blase <i>et al.</i> (1995) 1L	4.3	5.40	5.78	7.53
Blase <i>et al.</i> (1995) Cryst.	3.9	4.12, 6.33	≈ 5.8	≈ 7.4
Catellani <i>et al.</i> (1986) Cryst.	3.9	4.3, 6.7	6.2	7.4

TABLE 2. Band gap and valence band widths (all in eV) for monolayer (1L), bilayer (2L), and crystalline BN; all in eV. Note that the Blase *et al.* results cited are their LSDA (Ceperley-Alder), not GW, values. The two approximate values are taken from their Fig. 2. The experimental gap is a crystalline value from Hoffmann *et al.* (1984); the experimental band widths are for the 1L adsorbed on Ni(111) from Nagashima *et al.* (1995).

the experimental bands for the epitaxial monolayers on transition metal (111) surfaces argues strongly for the claim that the BN layer is indeed physisorbed in the experiments.

The “interlayer” states (states with density maxima in between BN planes) at the lowest unoccupied Γ -point [Catellani *et al.* (1986)], already are in evidence in the monolayer. That is, they are an intrinsic property of a solitary h -BN plane, and not essentially dependent on the confinement of two layers. The shape of their dispersion agrees well with the results found by Blase *et al.* (1995) in their supercell treatment of the BN sheet. The effective mass of those states is close to the free-electron mass, hence a tight-binding approximation description is poor [Robertson (1984)]. The corresponding quasi-particle energy bands of Kobayashi *et al.* (1994) are much higher in energy and even remain above the π^* band throughout the BZ. We follow Blase *et al.* (1995) in believing that this discrepancy is a consequence of the minimal basis set used by Kobayashi *et al.* (1994), leaving aside the question of the equivalence between KS and quasi-particle orbitals. We confirm the sensitivity with respect to basis set changes pointed out earlier [Vračko *et al.* (1990)] by trying a switch to the Tavouktsoglou & Huzinaga (1980) minimal basis set but with only the $1s$ orbital contracted. As a result, the LSDA gap between the two lowest unoccupied bands at the Γ -point grows to 5 eV.

The band structure of the bilayer is shown in Fig. 2 based on a calculation with 30×30 points in the full BZ. Upward dispersion near K along Γ -K again is found. As expected from the bulk crystalline value, the 2L bandgap is smaller than for the 1L (for reference, see the LSDA band structure of the crystal in Blase *et al.* (1995)). The gap is now indirect, that is, behavior which is qualitatively that of the bulk crystal appears even with only two planes of h -BN. Furthermore, the two π valence bands which first appear in the bilayer have widths close to those found by both Blase *et al.* (1995) and Catellani *et al.* (1986) for the crystal, another clear consequence of weak interplanar binding.

Simply because the monolayer has half as many atoms and electrons in the unit cell as the bilayer (or the crystal), what might appear to the uninitiated reader as a pseudo-degeneracy of the valence π -band at Γ in the monolayer is removed in the bilayer. Note that the two-dimensional band structures are not given, as Fig. 1 in the article by Rubio *et al.* (1994) suggests, by a simple clipping of the band structure of the three-dimensional crystal.

The B $1s$ level energy relative to the vacuum level shifts by 5.7 and 6 eV compared with the spin-split KS $1s_{\uparrow}$ and $1s_{\downarrow}$ states calculated for the spin-polarized isolated atom. The agreement with the experimental value, 4 eV, of this surface core-level shift [Hanke *et al.* (1990)] is rather good taking into account that our non-relativistic calcu-

D_{30}	-0.302042951149	D_{03}	-0.000559257071
D_{21}	0.008650353218	D_{12}	-0.034485592749
D_{20}	0.941267597296	D_{02}	0.046604929850
D_{11}	0.122372773515	D_{00}	-16.077200393719
a_e	9.007386003161	c_e	24.508023199574

TABLE 3. Non-zero parameters for the cubic function (4.1) used to fit $E(a, c)$ for sapphire around the calculated energy minimum; see text.

lations predict K -shell energies that are roughly 20 eV above the experimental values [Jia *et al.* (1996)] of -190.6 eV for B and -398.3 eV for N [Murray (1990)]. We obtain core-level shifts of the spin-split $1s$ shell of N of 4.0 and 5.8 eV.

4. Sapphire and computational requirements

Finally, to illustrate the computational opportunities for the LCGTO-FF method as embodied in the code GTOFF, we summarize recent results obtained by one of us [Boettger (1996)] on crystalline sapphire, α - Al_2O_3 . The crystal structure is rhombohedral with two formula units per primitive unit cell. Equivalently the structure may be treated as hexagonal with six formula units per cell and lattice parameters a and c , where c is the length of the primitive cell along the 3-fold axis. The positions of all ten atoms in the rhombohedral unit cell can be specified with two internal parameters; the distance in units of c from the origin to one of the Al atoms (u) and the distance in units of a from the c -axis to each O atom (v). Under ambient conditions, the lattice parameters [Wyckoff (1964)] are $a = 9.0008a_0$, $c = 24.572a_0$, $u = 0.352$, and $v = 0.306$.

Optimized values of $u = 0.352$ and $v = 0.306$, identical with experiment, were found for a and c fixed near the experimental values. Experimental evidence is that these two internal parameters are rather insensitive to pressure, so optimization of V (cell volume) and c/a proceeded at those values of u and v . The results near the energy minimum were fitted to a cubic form:

$$E(a, c) = \sum_{i=0}^3 \sum_{j=0}^{3-i} D_{ij} (a - a_e)^i (c - c_e)^j. \quad (4.1)$$

The non-zero constants are listed in Table 3 and the calculated results are compared with experiment and other calculations in Table 4. Clearly there is remarkably good agreement with experiment. Thus sapphire proves to be another example of a system for which LSDA folklore is not true: there is no meaningful bond contraction.

These calculations used segmented $6s3p1d$ Al and $5s3p1d$ O orbital (KS) bases respectively. The charge and XC fitting basis sets comprised 118 and 88 primitive GTOs per unit cell respectively. The calculations were done on a Sun SPARCstation 5 with 40 MBytes of real memory, 300 MBytes of swap space, and 1.5 GBytes total disk space. The integrals step for each geometry requires 160 MBytes of address space, runs for 5.5 hours, and requires roughly 300 MBytes of disk space. The corresponding scf step needs 72 MBytes of address space and runs about 14 minutes per iteration. Between 10 and 20 iterations are required for convergence, yielding about two completed geometries per day. Based on those data, plus corresponding experience with the Al 12-layer and a 21 atom-per-cell calculation for Na on Al(111), the current limit for GTOFF on a personal workstation is a reasonably symmetrical system with about 40 first- and second-row atoms or 20 $3d$ transition atoms per unit cell. On a single node of a truly top-end

Source	u	v	a	c	c/a	V_e
LCGTO (a)	0.354	0.304	8.955	24.61	2.748	284.88
OLCAO (b)	0.355	0.312	9.136	23.84	2.61	287.3
Present	0.352	0.306	9.0074	24.508	2.721	287.00
Expt. 293 K (c)	0.352	0.306	9.0059	24.585	2.730	287.81
Expt. 293 K (d)	0.352	0.306	9.0008	24.572	2.730	287.33
Expt. 100 K	9.0005	24.566	2.729	287.24

TABLE 4. Calculated and measured values for the internal lattice parameters (u and v), hexagonal cell lattice constants (a and c ; a_0), c/a ratio, and zero-pressure volume (V_e ; a_0^3 /molecule) of sapphire. References: (a) Salasco *et al.* (1991); (b) Ching & Xu (1994); (c) d'Amour *et al.* (1978); (d) Wyckoff (1964). Values at 100 K obtained from the room temperature data of d'Amour *et al.* (1978) by applying thermal expansion data from Touloukian *et al.* (1977).

machine this translates easily into 70–90 atoms per cell. For such large systems the decoupling of remote regions which takes place naturally in the LCGTO ansatz will lead to near-linear scaling. Parallelization, which we are about to undertake, will enable straightforward treatment of even more complex systems without resort to pseudo-potentials or explicitly “order- N ” schemes.

SBT and RJM were supported in part by the U. S. Army Office of Research under Grant No. DAA-HO4-95-1-0326. JCB's work was done under the auspices of the U. S. Dept. of Energy. Continuing collaboration with J. R. Sabin is acknowledged with pleasure and thanks.

Appendix A. Boron Nitride Basis Sets

The KS and fitting function basis sets are listed in Tables 5 and 6 respectively.

REFERENCES

- D'AMOUR, H., SCHIFERL, D., DENNER, W. SCHULZ, H. & HOLZAPFEL, W. B. 1978 High-pressure single-crystal structure determinations for ruby up to 90 kbar using an automatic diffractometer. *J. Appl. Phys.* **49**, 4411–4416.
- BLASE, X., RUBIO, A., LOUIE, S. G. & COHEN, M. L. 1995 Quasiparticle band structure of bulk hexagonal boron nitride and related systems. *Phys. Rev. B* **51**, 6868–6875.
- BOETTGER, J. C. 1993 Theoretical strain-dependent properties of square and hexagonal Fe monolayers. *Phys. Rev. B* **48**, 10247–10253.
- BOETTGER, J. C. 1995 Equation of state calculations using the LCGTO-FF method: equilibrium properties of hcp Beryllium. *Int. J. Quantum Chem.* **S29**, 197–202.
- BOETTGER, J. C. 1996 High-precision, all-electron, full-potential calculation of the equation of state and elastic constants of corundum. *Phys. Rev. B* (submitted).
- CATELLANI, A., POSTERNAK, M., BALDERESCHI, A., JANSEN, H. J. F. & FREEMAN, A. J. 1986 Electronic interlayer states in hexagonal boron nitride. *Phys. Rev. B* **32**, 6997–6999; Erratum *ibid.* **34**, 5929. CATELLANI, A., POSTERNAK, M., BALDERESCHI, A. & FREEMAN, A. J. 1987 Bulk and surface electronic structure of hexagonal boron nitride. *ibid.* **36**, 6105–6111.
- CAUSÁ, M., DOVESI, R., ORLANDO, R., PISANI, C. & SAUNDERS, V. R. 1988 Treatment of the exchange interactions in Hartree-Fock linear combination of atomic orbital calculations of periodic systems. *J. Phys. Chem.* **92**, 909–913. DOVESI, R., PISANI, C. & ROETTI, C. 1980 Exact-exchange Hartree-Fock calculations for periodic systems. II. Results for graphite and hexagonal boron nitride. *Int. J. Quantum Chem.* **17**, 517–529. DOVESI, R., PISANI,

boron orbital basis			nitrogen orbital basis		
type	exponent	contr. coeff.	type	exponent	contr. coeff.
<i>s</i>	10324.6500	0.0002454	<i>s</i>	73438.1890	0.0000507
<i>s</i>	1587.28340	0.0018662	<i>s</i>	11047.0972	0.0003934
<i>s</i>	358.646410	0.0099072	<i>s</i>	2502.42218	0.0020822
<i>s</i>	99.4211670	0.0415145	<i>s</i>	702.062923	0.0088571
<i>s</i>	31.5161170		<i>s</i>	225.293453	0.0319537
<i>s</i>	11.0921771		<i>s</i>	79.6158100	
<i>s</i>	4.22951829		<i>s</i>	30.2372830	
<i>s</i>	1.65726720		<i>s</i>	12.2636220	
<i>s</i>	0.426597528		<i>s</i>	5.26508600	
<i>s</i>	0.165131153		<i>s</i>	2.33347100	
<i>s</i>	0.0659908063		<i>s</i>	0.901856000	
$p_{x,y,z}$	24.4477348	0.0046651	<i>s</i>	0.360486016	
$p_{x,y,z}$	5.68465170	0.0310187	<i>s</i>	0.141903000	
$p_{x,y,z}$	1.83045908		$p_{x,y,z}$	126.996654	0.0011801
$p_{x,y,z}$	0.680498197		$p_{x,y,z}$	29.8373890	0.0094266
$p_{x,y,z}$	0.267382988		$p_{x,y,z}$	9.39403800	0.0440971
$p_{x,y,z}$	0.106316117		$p_{x,y,z}$	3.40510400	
p_z (1L)	0.0408781931		$p_{x,y,z}$	1.35810000	
			$p_{x,y,z}$	0.548914214	
			$p_{x,y,z}$	0.216172910	
			$p_{x,y,z}$	0.0804235652	

TABLE 5. Exponents and contraction coefficients for Hermite Gaussian type basis sets for the BN Kohn-Sham orbitals. (1L) means that the component was only used for the monolayer. The B basis is close to a Huzinaga & Sakai (1969) set and the N basis close to a van Duijneveldt (1971) set. The exponents here are changed to result in LSDA (HL) energies for the isolated atoms that are approximately $1 \cdot 10^{-4}$ Hartree lower than the energy from the published exponents (which optimize Hartree-Fock atomic energies).

type	boron fitting basis		nitrogen fitting basis	
	charge	exch.-corr. pot.	charge	exch.-corr. pot.
<i>s</i>	198.841332		450.584636	
<i>s</i>	63.0319164		159.230818	
<i>s</i>	22.1842424	7.39478466	60.4742613	20.1581885
<i>s</i>	8.45899396	2.81967883	24.5271204	8.17574792
<i>s</i>	3.31451770	1.10484479	10.5301189	3.51005730
<i>s</i>	0.853190758	0.284398349	4.66691849	1.55564732
<i>s</i>	0.330260643	0.110087434	1.80370291	0.601237327
<i>s</i>	0.131980948	0.0439938704	0.720968400	0.240324008
<i>s</i>			0.283804570	0.0946019991
p_z (2L)	1.10709572	1.10709572	3.69157100	3.69157100
p_z (2L)	0.432514141	0.432514141	1.45077021	1.45077021
p_z (2L)	0.172306923	0.172306923	0.576658920	0.576658920
$d_{z^2-(x^2+y^2)/2}$	3.66089972 (1L)	3.66089972	6.81017369 (1L)	6.81017369
$d_{z^2-(x^2+y^2)/2}$	1.36098954	1.36098954	2.71618632	2.71618632
$d_{z^2-(x^2+y^2)/2}$	0.534763282	0.534763282	1.09782290	1.09782290
$d_{z^2-(x^2+y^2)/2}$			0.432343642	0.432343642

TABLE 6. Exponents of Hermite Gaussian type functions for the BN fitting functions. *s*-type functions that obey the rules of Dunlap *et al.* (1979) are written in the same line.

- C., ROETTI, C. & SAUNDERS, V. R. 1983 Treatment of coulomb interactions in Hartree-Fock calculations of periodic systems. *Phys. Rev. B* **28**, 5781–5792. PISANI, C., DOVESI, R., NADA, R. & KANTOROVICH, L. N. 1990 Ab initio Hartree-Fock perturbed-cluster treatment of localized defects in crystals. *J. Chem. Phys.* **92**, 7448–7460.
- CHING, W. Y. & XU, Y. N. 1994 First-principles calculation of electronic, optical, and structural properties of α -Al₂O₃. *J. Amer. Ceram. Soc.* **77**, 404–411.
- COX, J. D., WAGMAN, D. D. & MEDVEDEV, V. A. 1989 *CODATA. Key Values for Thermodynamics*. Hemisphere.
- DONI, E. & PARRAVICINI, G. P. 1969 Energy bands and optical properties of hexagonal boron nitride and graphite. *Nuovo Cim.* **64**, 117–144.
- DUNLAP, B. I., CONOLLY, J. W. D., & SABIN, J. R. 1979 On some approximations in applications of $X\alpha$ theory. *J. Chem. Phys.* **71**, 3396–3402.
- VAN DUJINEVELDT, F. B. 1971, *IBM Research Report RJ945*.
- DWORKIN, A. S., SASMOR, D. J. & ARTSDALEN, E. R. VAN 1954 The thermodynamics of boron nitride; low temperature heat capacity and entropy; heats of combustion and formation. *J. Chem. Phys.* **22**, 837–842.
- FURTHMÜLLER, J., HAFNER, J. & KRESSE, G. 1995 Ab initio calculation of the structural and electronic properties of carbon and boron nitride using ultrasoft pseudopotentials. *Phys. Rev. B* **50**, 15606–15622.
- HANKE, G., KRAMER, M. & MÜLLER, K. 1990 Low energy Auger transmissions of *h*-BN and *c*-BN: An example of the influence of crystallographic structure on the Auger decay. p. 207–228 in Pouch & Alterovitz (1990).
- HERZBERG, G. 1950 *Molecular Spectra and Molecular Structure I. Spectra of Diatomic Molecules*. p. 512. Van Nostrand Reinhold.
- HOFFMANN, D. M., DOLL, G. L. & EKLUND, P. C. 1984 Optical properties of pyrolytic boron nitride in the energy range 0.05–10 eV. *Phys. Rev. B* **30**, 6051–6056.
- HUZINAGA, S. & SAKAI, Y. 1969 Gaussian-type functions for polyatomic systems II. *J. Chem. Phys.* **50**, 1371–1381.
- JIA, J. J., CALLCOTT, T. A., SHIRLEY, E. L., CARLISLE, J. A., TERMINELLO, L. J., ASFAW, A., EDERER, D. L., HIMPSEL, F. J. & PERERA, R. C. C. 1996 Resonant inelastic x-ray scattering in hexagonal boron nitride observed by soft-x-ray fluorescence spectroscopy. *Phys. Rev. Lett.* **76**, 4054–4057.
- KOBAYASHI, K., SANO, T. & I'HAYA, Y. J. 1994 Quasi-particle energy band structure and core-electron transition energy calculations for two-dimensional boron nitride. *Chem. Phys. Lett.* **219**, 53–56.
- LAM, P. K., WENTZCOVICH, R. M. & COHEN, M. L. 1990 High density phases of BN. In [Pouch & Alterovitz (1990)], pp. 165–192.
- LANDOLT, H. & BÖRNSTEIN, R. R. 1982 *Numerical Data and Functional Relationships in Science and Technology*, III/17a. pp. 150–152. Springer.
- LYNCH, R. W. & DRICKAMER, H. G. 1966 Effect of high pressure on the lattice parameters of diamond, graphite and hexagonal boron nitride. *J. Chem. Phys.* **44**, 181–184.
- MORUZZI, V. L., JANAK, J. F. & WILLIAMS, A. R. 1978 *Calculated Electronic Properties of Metals*. Pergamon. HEDIN, L. & LUNDQVIST, B. I. 1971 Explicit local exchange-correlation potentials. *J. Phys. C* **4**, 2064–2083.
- MURRAY, P. T. 1990 Growth of BN thin films by pulsed laser evaporation. p. 153–164 in Pouch & Alterovitz (1990).
- NAGASHIMA, A., TEJIMA, N., GAMOU, Y., KAWAI, T. & OSHIMA, C. 1995 Electronic dispersion relations of monolayer hexagonal boron nitride formed on the Ni(111) surface. *Phys. Rev. B* **51**, 4606. 1995 Electronic structure of monolayer hexagonal boron nitride physisorbed on metal surfaces. *Phys. Rev. Lett.* **75**, 3918–3921.
- NOZAKI, H. & ITOH, S. 1996 Lattice dynamics of BC₂N. *Phys. Rev. B* **53**, 14161–14170.
- PERDEW, J. P. & ZUNGER, A. 1981 Self-interaction correction to density-functional approximations for many-electron systems. *Phys. Rev. B* **23**, 5048–5079.

- POUCH, J. J. & ALTEROVITZ, S. A., Editors, 1990 *Synthesis and Properties of Boron Nitride*. Materials Science Forum 54&55. Trans Tech Publications.
- PEASE, R. S. 1952 An x-ray study of boron nitride. *Acta Cryst.* 5, 356-361.
- ROBERTSON, J. 1984 Electronic structure and core exciton of hexagonal boron nitride. *Phys. Rev. B* 29, 2131-2137. ZUNGER, A., KATZIR, A. & HALPERIN, A. 1976 Optical properties of hexagonal boron nitride. *ibid.* 13, 5560-5073.
- RUBIO, A., CORKILL, J. L. & COHEN, M. L. 1994 Theory of graphitic boron nitride nanotubes. *Phys. Rev. B* 49, 5081-5084. RUBIO, A., MIYAMOTO, Y., BLASE, X., COHEN, M. L., & LOUIE, S. G. 1996 Theoretical study of one-dimensional chains of metal atoms in nanotubes. *ibid.* 53, 4023-4026.
- SALASCO, L., DOVESI, R., CAUSÁ, M. & SAUNDERS, V. 1991 A periodic ab initio extended basis set study of α -Al₂O₃. *Molec. Phys.* 72, 267-277.
- SICHEL, E. K., MILLER, R. E., ABRAHAMS, M. S. & BUIOCCHI, C. J. 1976 Heat capacity and thermal conductivity of hexagonal pyrolytic boron nitride. *Phys. Rev. B* 13, 4607-4611.
- TAVOUKTSOGLU, A. N. & HUZINAGA, S. 1980 A new gaussian basis set for molecular calculations. *J. Chem. Phys.* 72, 1385-1391.
- TOULOUKIAN, Y. S., KIRBY, R. K., TAYLOR, R. E. & LEE, T. Y. R. 1977 *Thermophysical Properties of Matter. Vol. 13 Thermal Expansion: Molecular Solids*. p. 176. Plenum.
- TRICKEY, S. B., MÜLLER-PLATHE, F., DIERCKSEN, G. H. F. & BOETTGER, J. C. 1992 Interplanar binding and lattice relaxation in a graphite dilayer. *Phys. Rev. B* 45, 4460-4468.
- TRICKEY, S. B. 1996 Benchmark comparison of gradient dependent and local density calculations for bulk silicon and aluminum. *Int. J. Quantum Chem.* (accepted).
- VRAČKO, M., LIEGENER, C.-M. & LADIK, J. 1990 Quasiparticle band structure and exciton spectrum of hexagonal boron nitride using second-order Møller-Plesset many-body perturbation theory. *Int. J. Quantum Chem.* 37, 241-248.
- WACHTERS, A. J. H. 1970 Gaussian basis set for molecular wavefunctions containing third-row atoms. *J. Chem. Phys.* 52, 1033-1036.
- WENTZCOVITCH, R. M., FAHY, S., COHEN, M. L. & LOUIE, S. G. 1988 Ab initio study of graphite \rightarrow diamondlike transitions in BN. *Phys. Rev. B* 38, 6191-6195.
- WYCKOFF, R. W. G. 1964 *Crystal Structures*, 2nd Ed., Vol. 2, p. 6. Interscience.